Supporting information

Physico-chemo-electrochemically coupled stable interface for high-capacity and durable aqueous zinc metal batteries

Gege Wang[a,b], Feifan Zhang[a,b], Caiyu Ma[c], Jianhua Yang[a], Xiaowei Chi[a,], Yu Liu [a,*]*

[a] Shanghai Institute of Ceramics, Chinese Academy of Sciences, Shanghai 200050, China
[b] University of Chinese Academy of Sciences, Beijing 100049, China
[c] School of Materials Science and Engineering, Shanghai University of Engineering Science, Shanghai 201620, China

* Corresponding author. Email: xwchi@mail.sic.ac.cn
* Corresponding author. Email: yuliu@mail.sic.ac.cn

The relationship between R_{ct} and the E_a follows the below Arrhenius equation:

$$\ln(R_{ct}^{-1}) = \ln A - E_a/RT$$

The E_a can be obtained by testing the temperature-dependent electrochemical impedance spectroscopy (EIS) of Zn//Zn symmetric cells. The EIS data for the cells with 2 M $ZnSO_4$ and 1% $EMIMBF_4$-added 2 M $ZnSO_4$ electrolytes under various temperatures are shown Table S1 and Table S2, respectively.

Table S1. EIS spectra of the Zn//Zn symmetric cells in 2 M $ZnSO_4$ at different temperatures.

Temperature [°C]	Temperature [K]	R_{ct} [Ω]	E_a [kJ mol^{-1}]
30	303.15	535.99	-2.73
40	313.15	210.00	-2.32
50	323.15	71.70	-1.86
60	333.15	20.60	-1.31
70	343.15	7.85	-0.89

Table S2. EIS spectra of the Zn//Zn symmetric cells in 2 M $ZnSO_4$+1% $EMIMBF_4$ at different temperatures.

Temperature [°C]	Temperature [K]	R_{ct} [Ω]	E_a [kJ mol^{-1}]
30	303.15	978.90	-2.99
40	313.15	409.64	-2.61
50	323.15	189.39	-2.28
60	333.15	92.08	-1.96
70	343.15	48.38	-1.68

Table S3. Comparison of the performance of Zn//Zn symmetric cells above a current density of 5 mA cm^{-2} and above an areal capacity of 5 mAh cm^{-2} with ionic liquid as additives in different research.

Additive	Current density [mA cm^{-2}]	Areal capacity [mAh cm^{-2}]	Cycle life [h]	Cumulative areal capacity [mAh cm^{-2}]
BMIM/ZTFO[1]	5	25	100	1250
ImS/ZSO[2]	10	20	350	3600
PZIL[3]	8	8	300	1200
HMIM/ZSO[4]	8	8	250	1000
PVIPS-1[5]	7.5	7.5	400	1500
PVIPS-2[5]	5	5	500	1250
This work	5	5	1200	3000

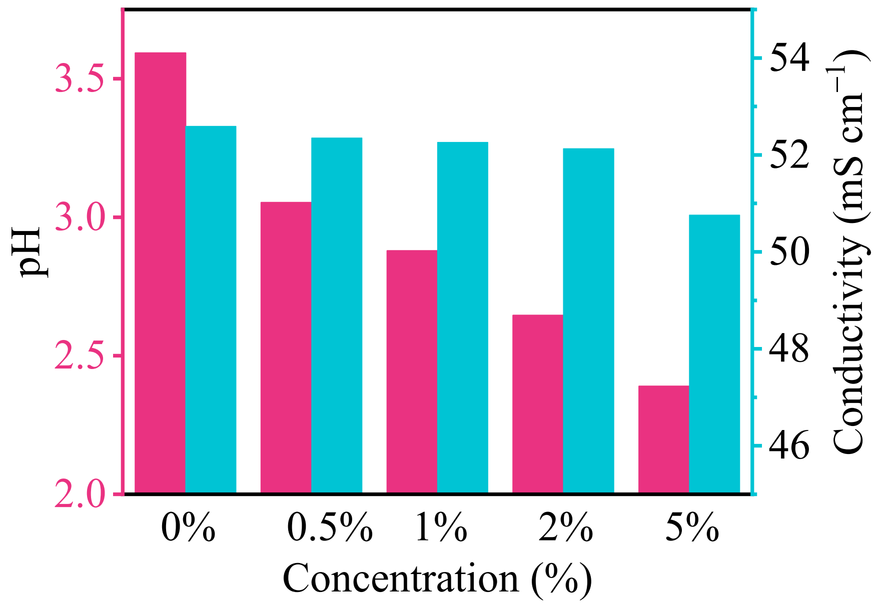

Figure S1. pH and conductivity of the electrolytes containing different concentrations of $EMIMBF_4$ (0%, 0.5%, 1%, 2% and 5%) additive.

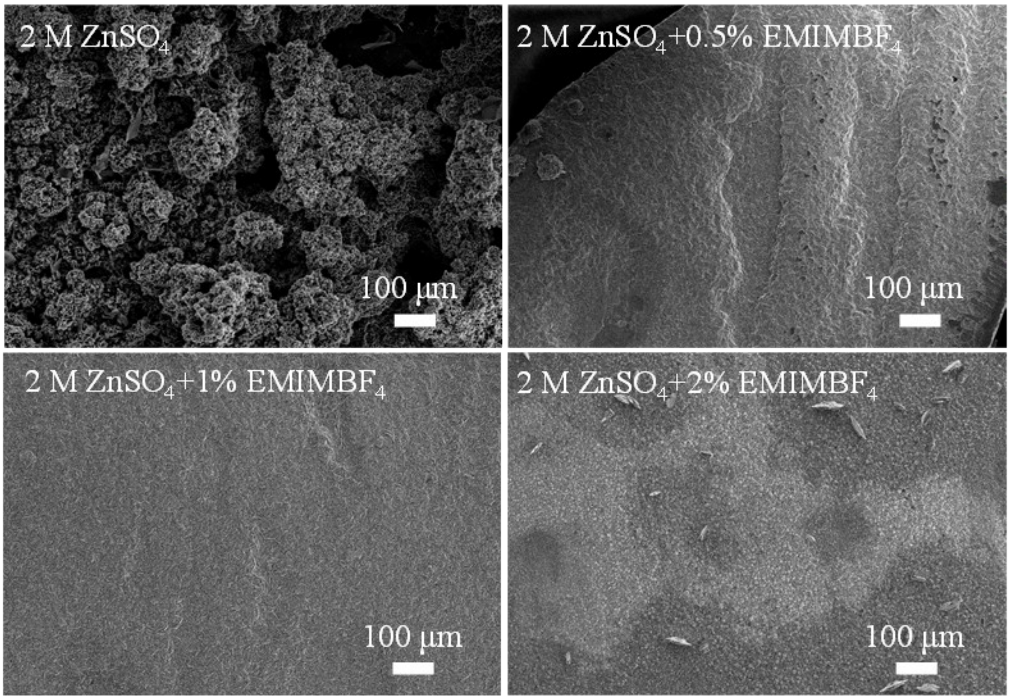

Figure S2. SEM images of the zinc electrode cycled in different electrolytes containing a series of concentrations of $EMIMBF_4$ (0%, 0.5%, 1% and 2%) additive.

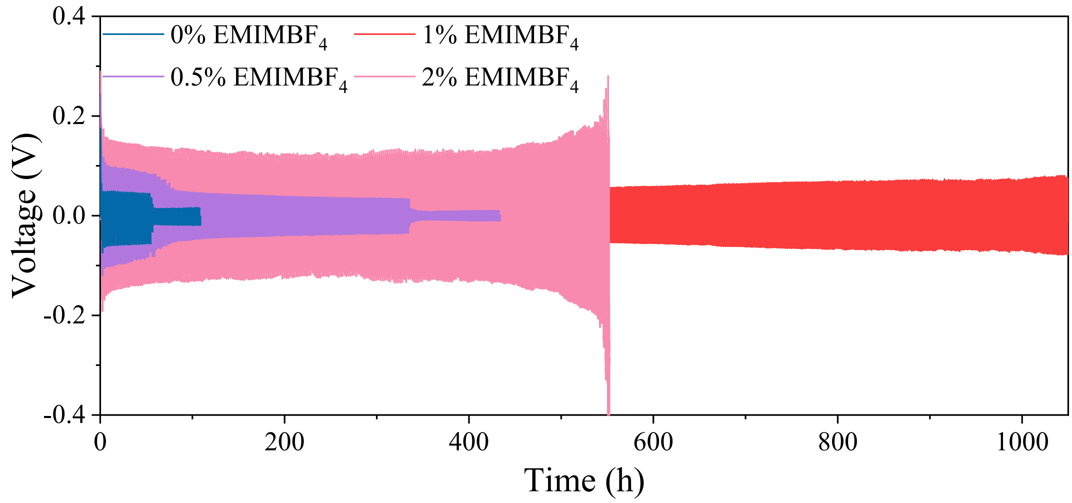

Figure S3. Voltage profiles of Zn//Zn symmetric cells with different electrolytes cycled at 5 mA cm^{-2} and 5 mAh cm^{-2}.

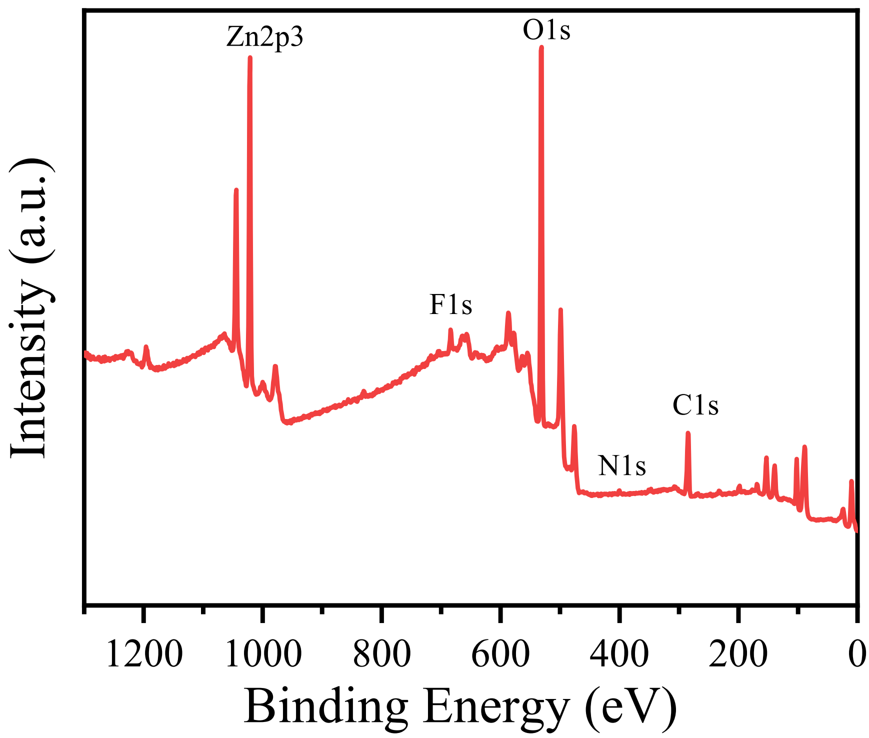

Figure S4. XPS survey spectrum of the cycled Zn electrode at 5 mA cm^{-2} and areal capacity of 5 mAh cm^{-2} after 50 cycles.

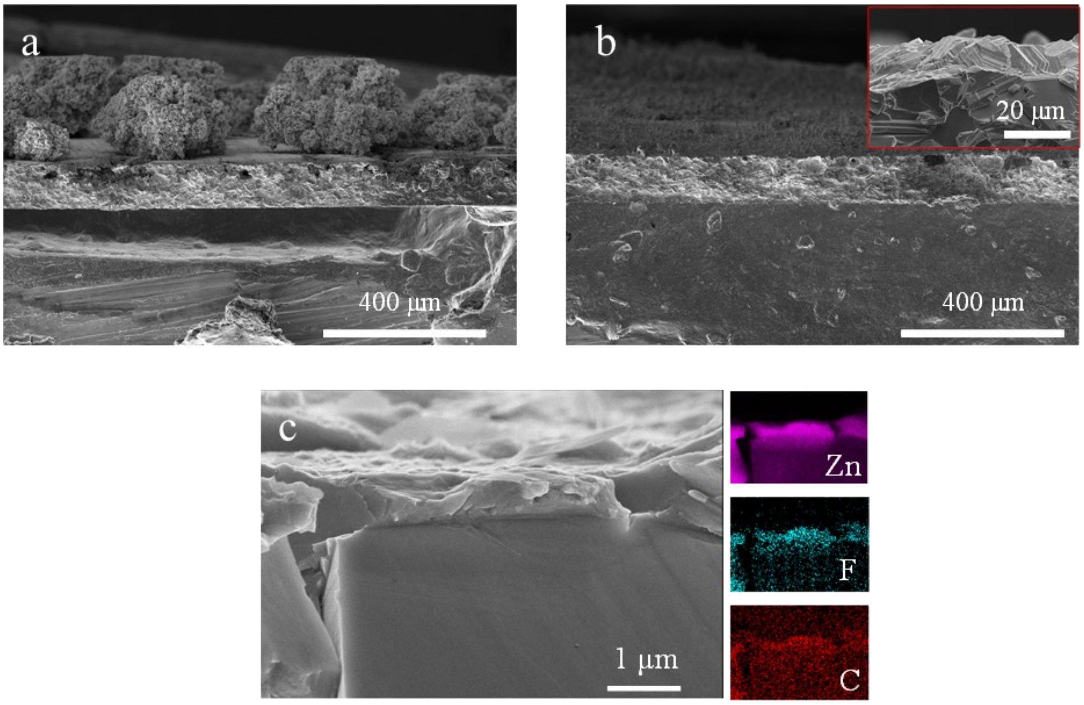

Figure S5. Cross-sectional SEM of the zinc electrode cycled in electrolyte (a) without and (b) with $EMIMBF_4$. (c) EDS images of the Zn electrode cycled in Zn//Zn symmetric cells at 5 mA cm^{-2} and 5 mAh cm^{-2} for 24 h.

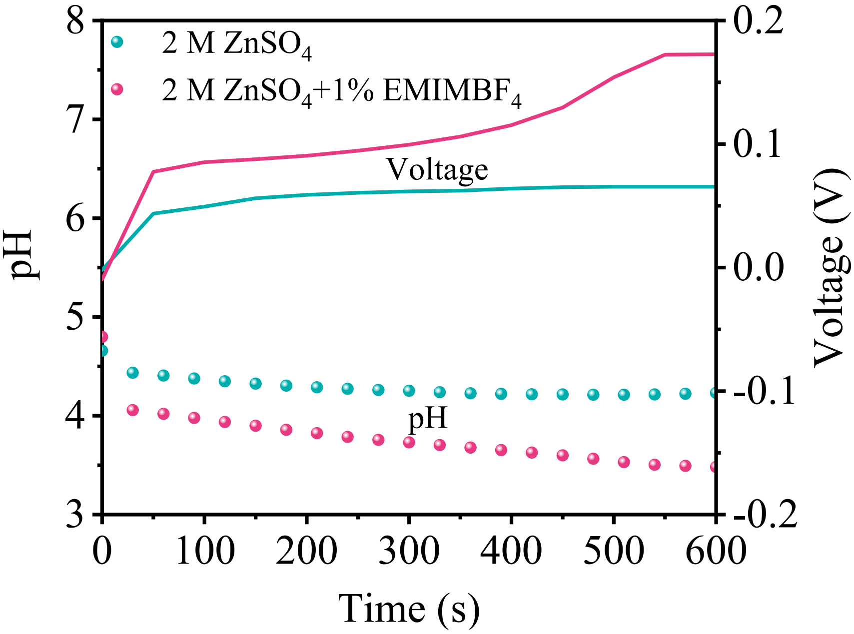

Figure S6. In-situ monitoring of the pH close to the Zn electrode surface during stripping.

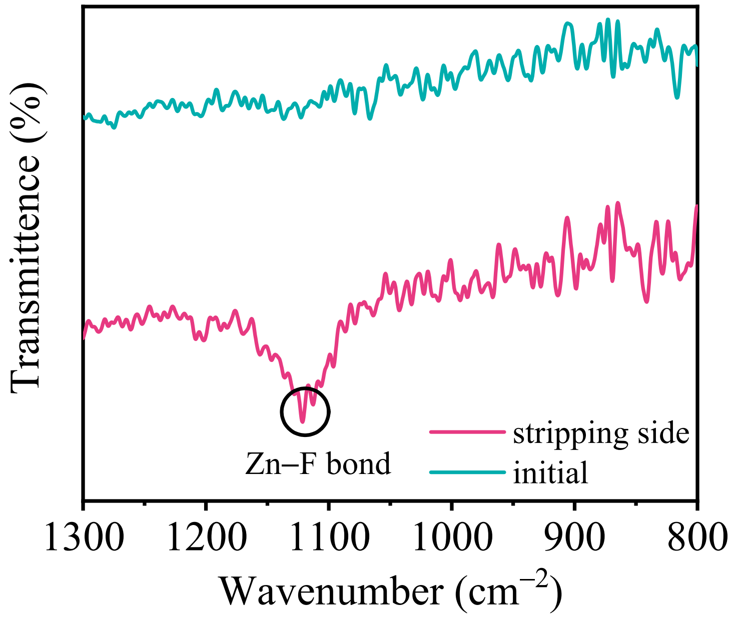

Figure S7. FTIR spectrum of the initial Zn foil and the Zn foil surface after stripping in the $EMIMBF_4$-added electrolyte.

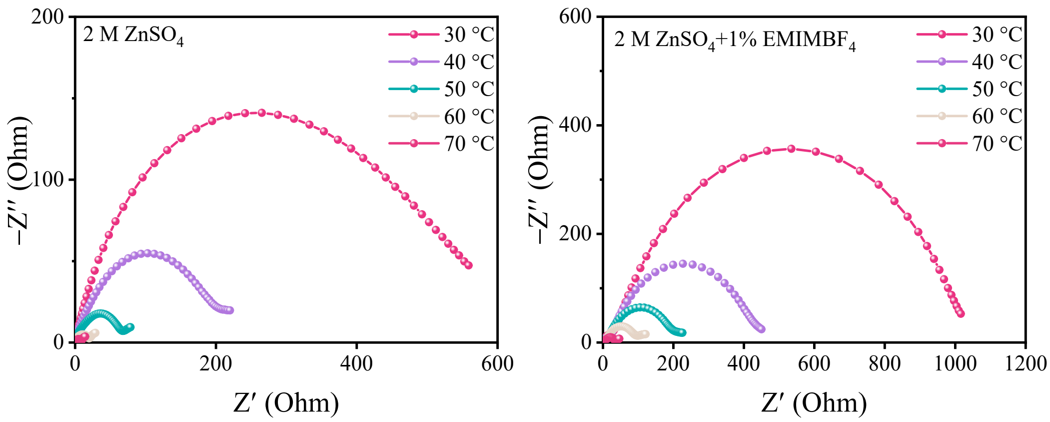

Figure S8. EIS spectra of the Zn//Zn symmetric cells at different temperatures in (a) 2 M $ZnSO_4$ and (b) 2 M $ZnSO_4$+1% $EMIMBF_4$.

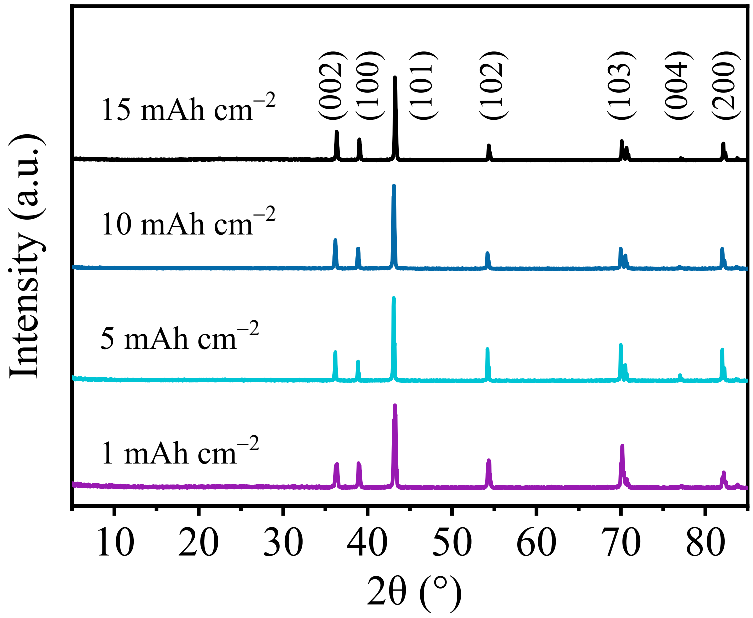

Figure S9. XRD patterns of different accumulative cycling capacity of zinc electrode under 5 mA cm^{-2} in 2 M $ZnSO_4$.

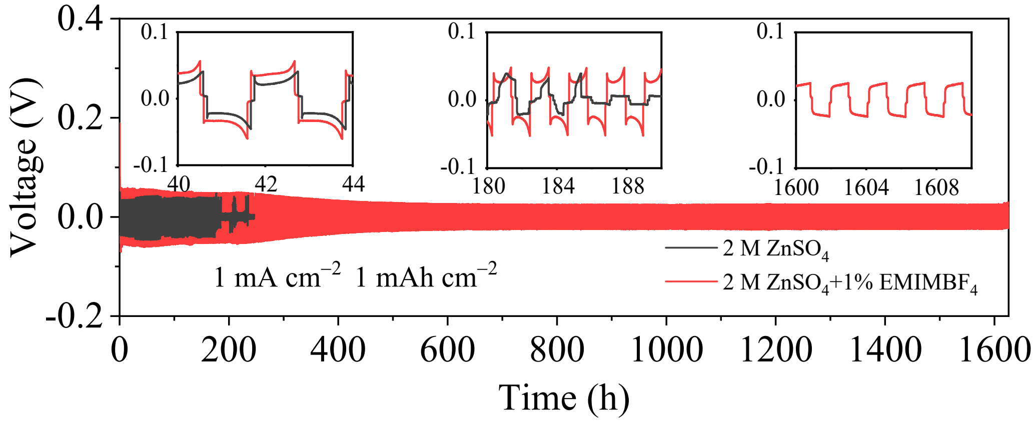

Figure S10. Long-term galvanostatic cycling of Zn//Zn symmetric cells with different electrolytes at 1 mA cm^{-2} and 1 mAh cm^{-2}.

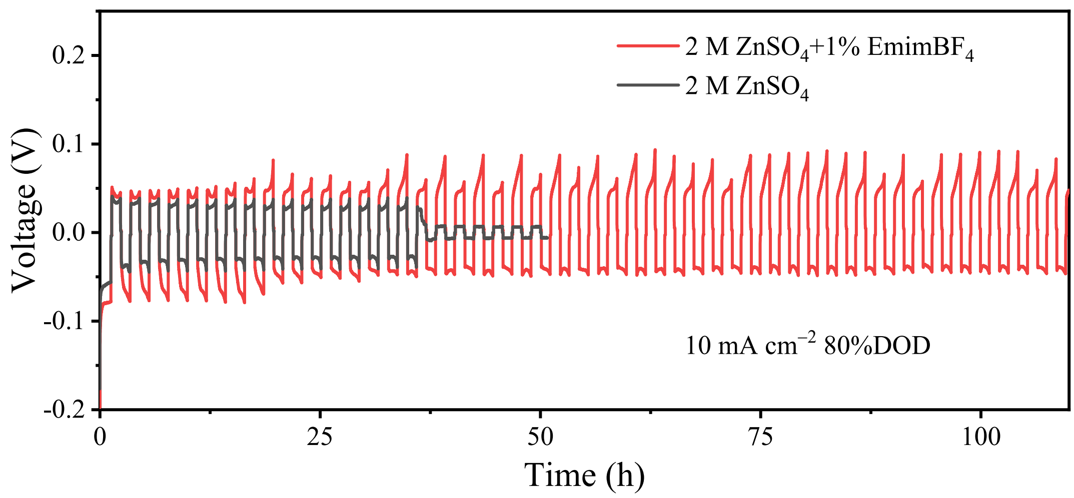

Figure S11. Galvanostatic cycling of Zn//Zn symmetric cells at 10 mA cm^{-2} and 80% DOD.

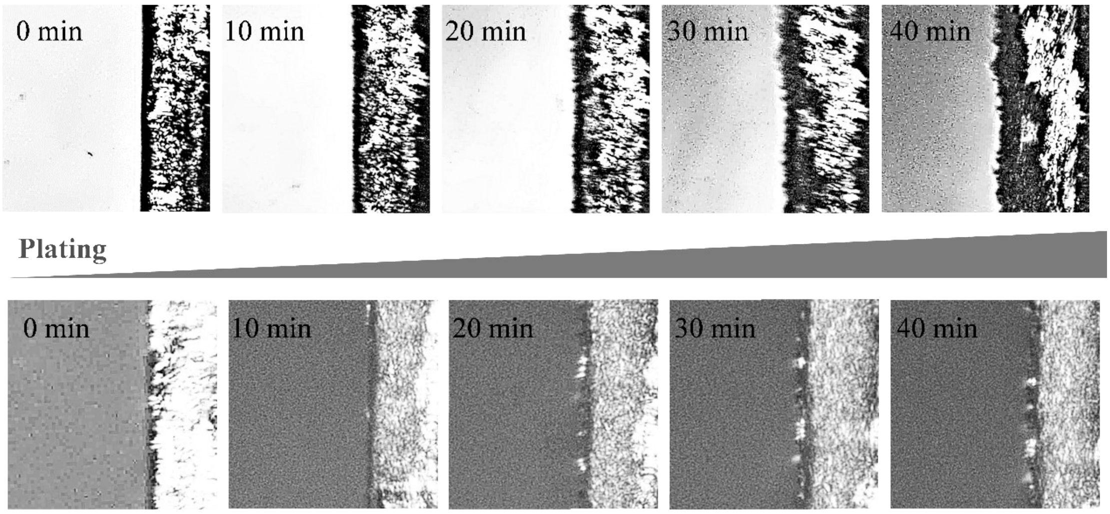

Figure S12. In-situ optical microscopic images of the evolution of the Zn deposition process zinc on a copper under a current density of 5 mA cm^{-2} from 0 min to 40 min.

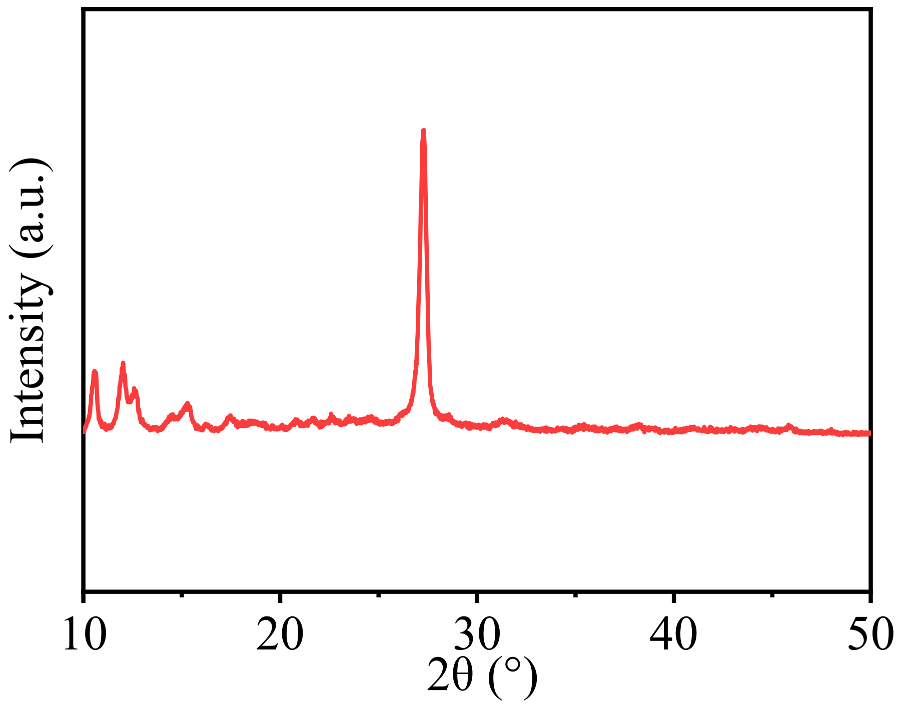

Figure S13. XRD pattern of HATNQ cathode powder.

References

1 J. Chen, W. Zhou, Y. Quan, B. Liu, M. Yang, M. Chen, X. Han, X. Xu, P. Zhang and S. Shi, *Energy Storage Materials*, 2022, **53**, 629–637.

2 Y. Lv, M. Zhao, Y. Du, Y. Kang, Y. Xiao and S. Chen, *Energy Environ. Sci.*, 2022, **15**, 4748–4760.

3 R. Chen, Q. Liu, L. Xu, X. Zuo, F. Liu, J. Zhang, X. Zhou and L. Mai, *ACS Energy Lett.*, 2022, **7**, 1719–1727.

4 C. Wu, C. Sun, K. Ren, F. Yang, Y. Du, X. Gu, Q. Wang and C. Lai, *Chemical Engineering Journal*, 2023, **452**, 139465.

5 Y. Hao, D. Feng, L. Hou, T. Li, Y. Jiao and P. Wu, *Advanced Science*, 2022, **9**, 2104832.